CSETS: 25
DEVELOPMENTS AND APPLICATIONS IN COMPUTATIONAL STRUCTURES TECHNOLOGY

Edited by: B.H.V. Topping, J.M. Adam, F.J. Pallarés, R. Bru and M.L. Romero

Chapter 1

Computational Advances in Masonry Structures: From Mesoscale Modelling to Engineering Application

P.B. Lourenço[1], D.V. Oliveira[1] and G. Milani[2]

[1]ISISE, Department of Civil Engineering, School of Engineering, University of Minho, Azurém, Guimaraes, Portugal
[2]Department of Structural Engineering, Politecnico di Milano, Italy

doi:10.4203/csets.25.1

Abstract

Masonry is a composite material that can be defined as a material incorporating a visible internal structure and having a low strength in tension. The latter characteristic has shaped most civil engineering structures up to the advent of reinforced concrete and iron/steel. The paper will detail two separate modelling issues: micro-modelling and homogenisation techniques, which represent both a popular and active field on masonry research; the engineering use of sophisticated numerical modelling, using one emblematic case study on a heritage structure, which poses significant challenges for practitioners.

Keywords: masonry, non-linear analysis, micro-modelling, homogenization, engineering applications.

1 Introduction

Masonry is a building material that has been used for more than ten thousand years. In many countries, masonry structures still amount to 30 to 50% of the new housing developments. Also, most structures built before the 19th century and still surviving are built with masonry. Research in the field is essential to understand masonry behaviour, to develop new products, to define reliable approaches to assess the safety level and to design potential retrofitting measures. To achieve these purposes, researchers have been trying to convert the highly indeterminate and non-linear behaviour of masonry buildings into something that can be understood with an acceptable degree of mathematical certainty. The fulfilment of this objective is complex and burdensome, demanding a considerable effort centred on integrated research programs, able to combine experimental research with the development of consistent constitutive models.

Masonry is usually described as a composite material formed by units and joint, with or without mortar, and different bond arrangements. It is certain that the

problems associated with modelling ancient and modern masonry structures are very different. Physical evidence shows us that ancient masonry is a very complex material with three-dimensional internal arrangement, usually unreinforced, but which can include some form of traditional reinforcement, whereas modern masonry is made usually with a regular arrangement of masonry units, with or without steel reinforcement, see Figure 1.

Figure 1: Examples of different masonry types (from left to right): timber braced "Pombalino" system emerging after the 1755 earthquake in Lisbon; irregular stone wall with a complex transverse cross section (18th century, Northern Portugal); typical European unreinforced masonry used in areas of low seismicity using thick blocks to comply with thermal and sound regulations.

The relevance of the internal structure of masonry in the structural response has been demonstrated. Figure 2 shows results in dry stone shear joints by Lourenço and Ramos [1], made with the same stone but with different surfaces treatments. The results indicate that, even for the same material, the friction and dilatancy angles are very dependent on the roughness of the joint. In particular, a smooth (polished) surface exhibits very low friction, compared with a sawn surface and a rough (artificially induced by a spike) surface. Smooth and sawn surfaces exhibit almost zero dilatancy, whereas a rough surface exhibits a negative non-negligible dilatancy angle. Similarly, Figure 3 shows results in masonry stone walls with the same geometry, subjected to combined vertical and cyclic horizontal in-plane loading, see Vasconcelos and Lourenço [2]. Three types of walls are considered, namely dry stone (without mortar), and coursed and rubble stone masonry with the same mortar. The results indicate that, despite the fact that the geometry is the same for all walls, different failure modes, ultimate lateral strength and hysteretic behaviour is found for the walls.

The fact that masonry has so much variability in materials and technology makes the computational modelling of masonry structures complex. This paper addresses, first, two possibilities to incorporate the internal structure of masonry in the constitutive model, be it by explicitly considering it or by the mathematical process of homogenization. Secondly, an emblematic case study of using advanced computations for engineering applications is presented.

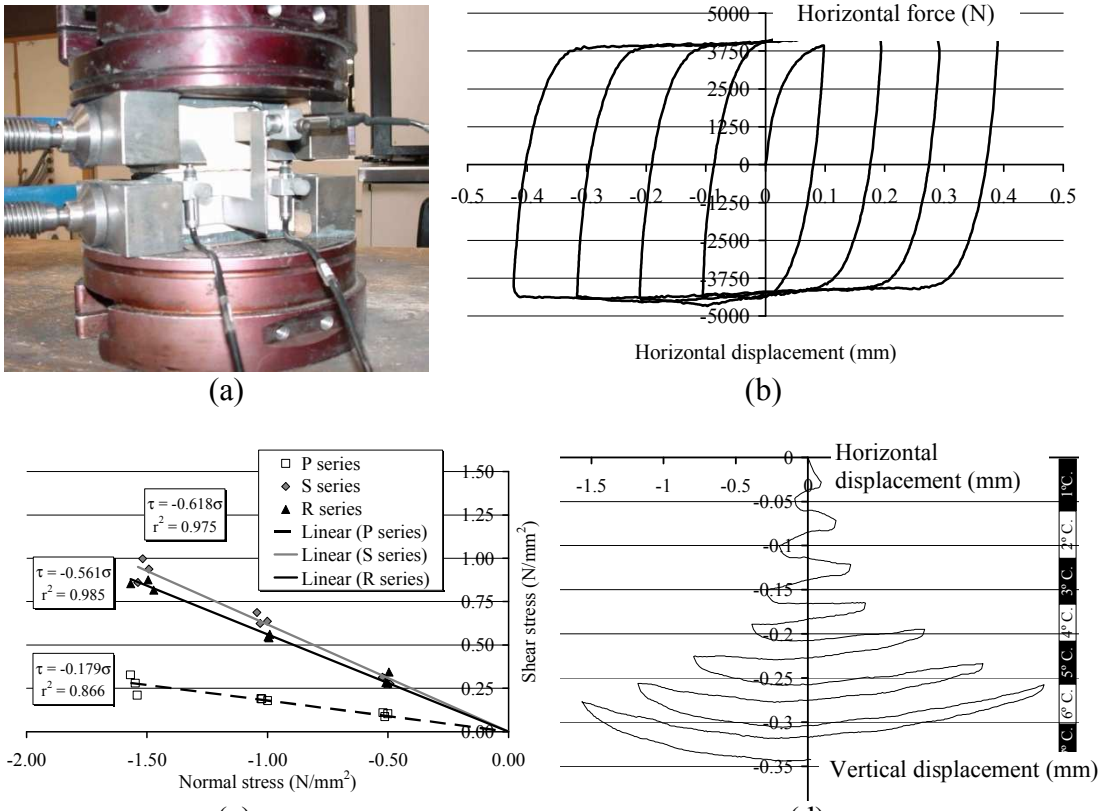

Figure 2: Behaviour of dry stone masonry joints under shear: (a) test set-up; (b) typical shear response in terms of horizontal force vs. displacement; (c) Coulomb envelop for (P)olished, (S)awn and (R)ough stone surfaces; (d) negative dilatancy (horizontal vs. vertical displacement) for rough stone surfaces.

2 Modelling Approaches

In general, the approach towards the numerical representation of masonry can focus on the micro-modelling of the individual components, viz. unit (brick, block, etc.) and mortar, or the macro-modelling of masonry as a composite, Rots [3]. Depending on the level of accuracy and the simplicity desired, it is possible to use the following modelling strategies, see Figure 4: (a) Detailed micro-modelling, in which units and mortar in the joints are represented by continuum elements whereas the unit-mortar interface is represented by discontinuous elements; (b) Simplified micro-modelling, in which expanded units are represented by continuum elements whereas the behaviour of the mortar joints and unit-mortar interface is lumped in discontinuous elements; (c) Macro-modelling, in which units, mortar and unit-mortar interface are smeared out in a homogeneous continuum.

(a)

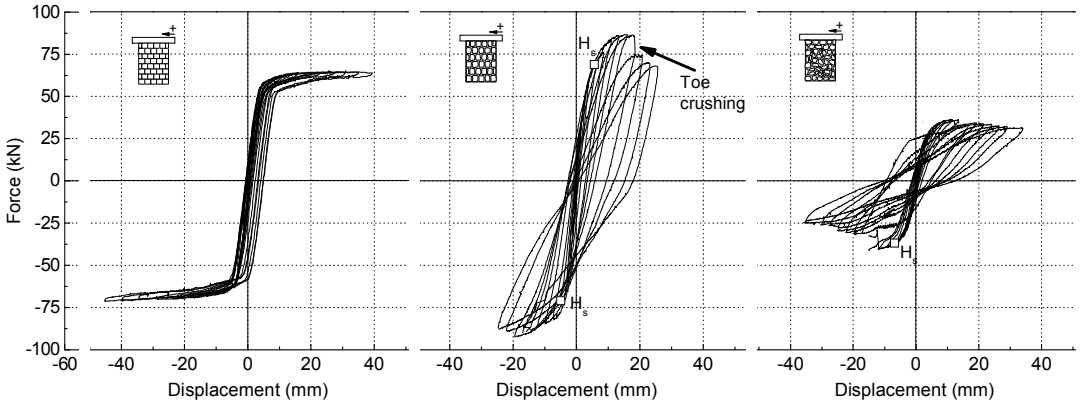

(b)

Figure 3: Experimental results on stone masonry shear walls: (a) failure mechanisms; (b) force-displacements diagrams. Note that the vertical load is not the same for all walls.

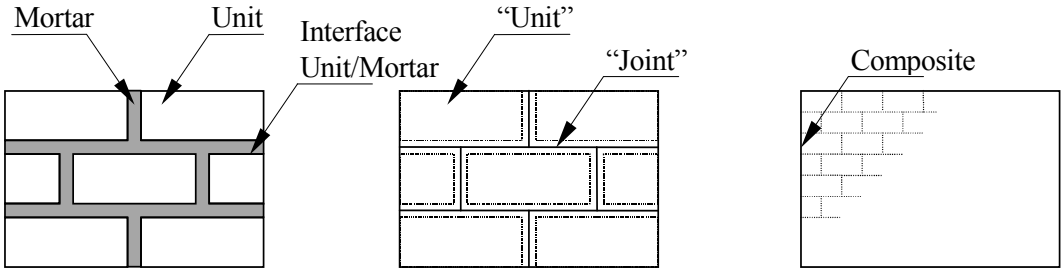

(a) (b) (c)

Figure 4: Modelling strategies for masonry structures: (a) detailed micro-modelling; (b) simplified micro-modelling; (c) macro-modelling.

In the first approach, Young's modulus, Poisson's ratio and, optionally, inelastic properties of both unit and mortar are taken into account. The interface represents a potential crack/slip plane with initial dummy stiffness to avoid interpenetration of the continuum. This enables the combined action of unit, mortar and interface to be

studied under a magnifying glass. In the second approach, each joint, consisting of mortar and the two unit-mortar interfaces, is lumped into an average interface while the units are expanded in order to keep the geometry unchanged. Masonry is thus considered as a set of blocks bonded by potential fracture/slip lines at the joints. Some accuracy is lost since Poisson's effect of the mortar is not included. The third approach does not make a distinction between individual units and joints but treats masonry as a homogeneous anisotropic continuum. Much effort is made today in the link between the micro- and macro-modelling approaches using homogenization techniques. One modelling strategy cannot be preferred over the other because different application fields exist for micro- and macro-models. Micro-modelling studies are necessary to give a better understanding about the local behaviour of masonry structures. Macro-modelling and homogenization studies are more adequate for engineering applications.

3 Modelling the Internal Structure

3.1 Micro-modelling

Different approaches are possible to represent heterogeneous media, namely, the discrete element method (DEM), the discontinuous finite element method (FEM) and limit analysis (LAn).

The typical characteristics of discrete element methods are: (a) the consideration of rigid or deformable blocks (in combination with FEM); (b) connection between vertices and sides / faces; (c) interpenetration is usually possible; (d) integration of the equations of motion for the blocks (explicit solution) using the real damping coefficient (dynamic solution) or artificially large (static solution). The main advantages are an adequate formulation for large displacements, including contact update, and an independent mesh for each block, in case of deformable blocks. The main disadvantages are the need of a large number of contact points required for accurate representation of interface stresses and a rather time consuming analysis, especially for 3D problems. Masonry applications can be found in Lemos [4].

The finite element method remains the most used tool for numerical analysis in solid mechanics and an extension from standard continuum finite elements to represent discrete joints was developed in the early days of non-linear mechanics. Interface elements were initially employed in concrete and rock mechanics, being used since then in a great variety of structural problems. A complete micro-model must include all the failure mechanisms of masonry, namely, cracking of joints, sliding over one head or bed joint, cracking of the units and crushing of masonry, as done in Lourenço and Rots [5] for monotonic loading and Oliveira and Lourenço [6] for cyclic loading.

Computational limit analysis received far less attention from the technical and scientific community for blocky structures. Still, limit analysis has the advantage of being a simple tool, while having the disadvantages that only collapse load and collapse mechanism can be obtained and loading history can hardly be included. A limit analysis constitutive model for masonry that incorporates non-associated flow

at the joints, tensile, shear and compressive failure and a novel formulation for torsion is given in Orduña and Lourenço [7,8].

Here, as an example of the possibilities that can be achieved with micro-modeling, a powerful interface model is detailed and applied to illustrative examples.

3.1.1 Implementation of a cyclic interface model

A relation between generalized stress and strain vectors is usually expressed as

$$\boldsymbol{\sigma} = \mathbf{D}\,\boldsymbol{\varepsilon} \tag{1}$$

where **D** represents the stiffness matrix. For zero-thickness line interface elements, the constitutive relation defined by Equation (1) expresses a direct relation between the traction vector and the relative displacement vector along the interface, which reads

$$\boldsymbol{\sigma} = \begin{Bmatrix} \sigma \\ \tau \end{Bmatrix} \quad \text{and} \quad \boldsymbol{\varepsilon} = \begin{Bmatrix} \Delta u_n \\ \Delta u_t \end{Bmatrix} \tag{2}$$

A constitutive interface model can be defined by a convex composite yield criterion, see Figure 5, composed by three individual yield functions, usually with softening included for all modes so that experimental observations can be replicated, reading

$$\begin{aligned} &\text{Tensile criterion: } f_t(\boldsymbol{\sigma}, \kappa_t) = \sigma - \bar{\sigma}_t(\kappa_t) \\ &\text{Shear criterion: } f_s(\boldsymbol{\sigma}, \kappa_s) = |\tau| + \sigma \tan\phi - \bar{\sigma}_s(\kappa_s) \\ &\text{Compressive criterion: } f_c(\boldsymbol{\sigma}, \kappa_c) = \left(\boldsymbol{\sigma}^T \mathbf{P} \boldsymbol{\sigma}\right)^{1/2} - \bar{\sigma}_c(\kappa_c) \end{aligned} \tag{3}$$

Here, ϕ represents the friction angle and **P** is a projection diagonal matrix, based on material parameters. $\bar{\sigma}_t$, $\bar{\sigma}_s$ and $\bar{\sigma}_c$ are the isotropic effective stresses of each of the adopted yield functions, ruled by the scalar internal variables κ_t, κ_s and κ_c.

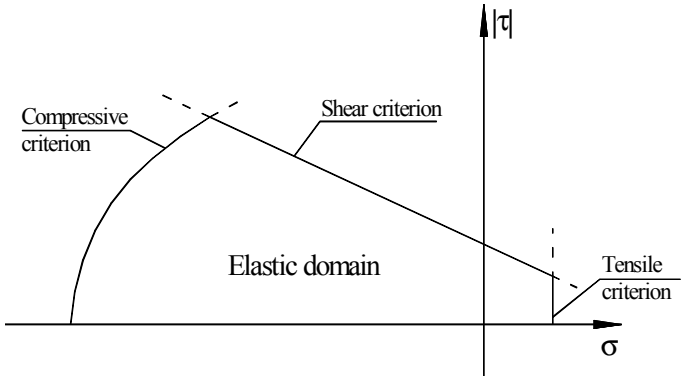

Figure 5: Multisurface interface constitutive model.

In order to include unloading/reloading behaviour in an accurate manner, an extension of the plasticity theory is addressed in Oliveira and Lourenço [6]. Two new auxiliary yield surfaces (termed unloading surfaces) similar to the monotonic ones were introduced in the monotonic model, so that unloading to tension and to compression could be modelled. Each unloading surface moves inside the admissible stress space towards the similar monotonic yield surface. In a given unloading process, when the stress point reaches the monotonic yield surface, the surface used for unloading becomes inactive and the loading process becomes controlled by the monotonic yield surface. Similarly, if a stress reversal occurs during an unloading process, a new unloading surface is started, subsequently deactivated when it reaches the monotonic envelope or when a new stress reversal occurs. The proposed model comprises six possibilities for unloading/reloading movements.

Unloading/reloading to tension can be started from any allowable stress point, except from points on the monotonic tensile surface, see Figure 6a, ruled according to the yield function

$$f_{Ut}(\boldsymbol{\sigma},\boldsymbol{\alpha},\kappa_{Ut}) = \boldsymbol{\xi}(1) - \bar{\sigma}_{i,Ut}(\gamma\kappa_{Ut}) \tag{4}$$

where $\boldsymbol{\alpha}$ is the back-stress vector, $\bar{\sigma}_{i,Ut}$ is the isotropic effective stress and κ_{Ut} is the tensile unloading hardening parameter. The scalar γ provides the proportion of isotropic and kinematic hardening. The relative (or reduced) stress vector $\boldsymbol{\xi}$ is given by

$$\boldsymbol{\xi} = \boldsymbol{\sigma} - \boldsymbol{\alpha} \tag{5}$$

In the same way, unloading/reloading to compression can take place from any acceptable stress point, except from points on the monotonic compressive surface, see Figure 6b, being controlled by the following yield function

$$f_{Uc}(\boldsymbol{\sigma},\boldsymbol{\alpha},\kappa_{Uc}) = \left(\boldsymbol{\xi}^T\mathbf{P}\boldsymbol{\xi}\right)^{1/2} - \bar{\sigma}_{i,Uc}(\gamma\kappa_{Uc}) \tag{6}$$

where $\bar{\sigma}_{i,Uc}$ is the isotropic effective stress and κ_{Uc} is the compressive unloading hardening parameter.

For each of the six hypotheses considered for unloading movements, a curve that relates the unloading hardening parameter κ_U and the unloading effective stress $\bar{\sigma}_U$ must be defined. Thus, the adoption of appropriate evolution rules makes possible to reproduce non-linear behaviour during unloading. Physical reasons imply that C^1 continuity must be imposed on all the six curves. Also, all functions must originate positive effective stress values, their derivatives must always be non-negative and its shape must be adequately chosen to fit experimental data, obtained from uniaxial tests. The six different curves adopted in this study are used in the

definition of the isotropic and kinematic hardening laws. The definition of the hardening laws requires material parameters, which allow to obtain numerical responses similar to experimental observations, see Figure 7. Aspects related to the algorithm can be found in Oliveira and Lourenço [6].

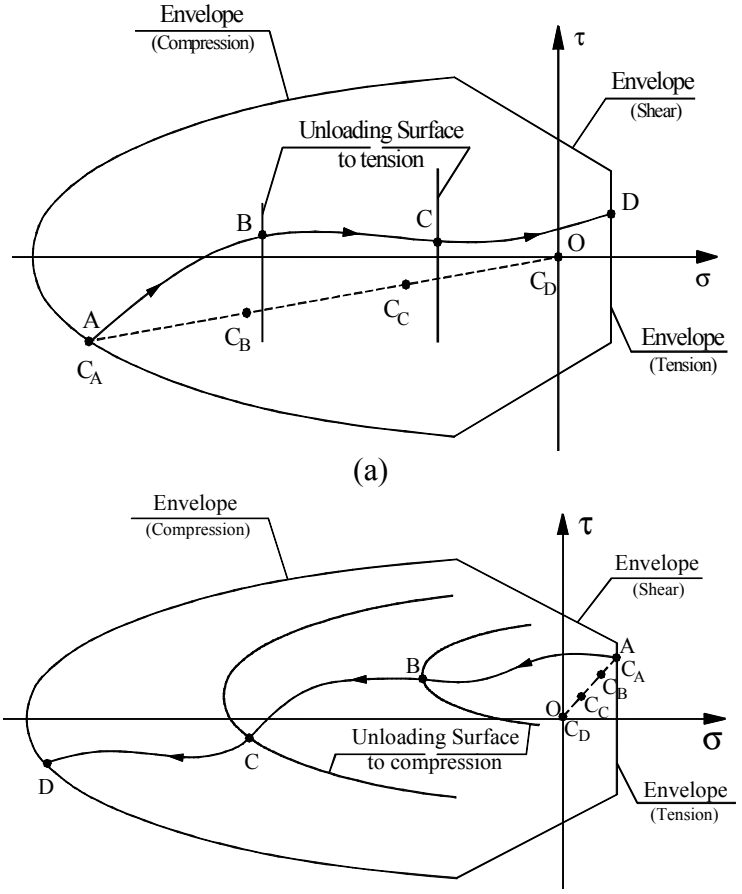

Figure 6: Hypothetic motion of the unloading surface in stress space to: (a) tension and to (b) compression.

3.1.2 Results

The ability of the model to reproduce the main features of structural masonry elements is now assessed through the numerical analysis of masonry walls submitted to cyclic loads, see Figure 8. In these simulations, the units were modelled using eight-node continuum plane stress elements with Gauss integration and, for the joints, six-node zero-thickness line interface elements with Lobatto integration were used.

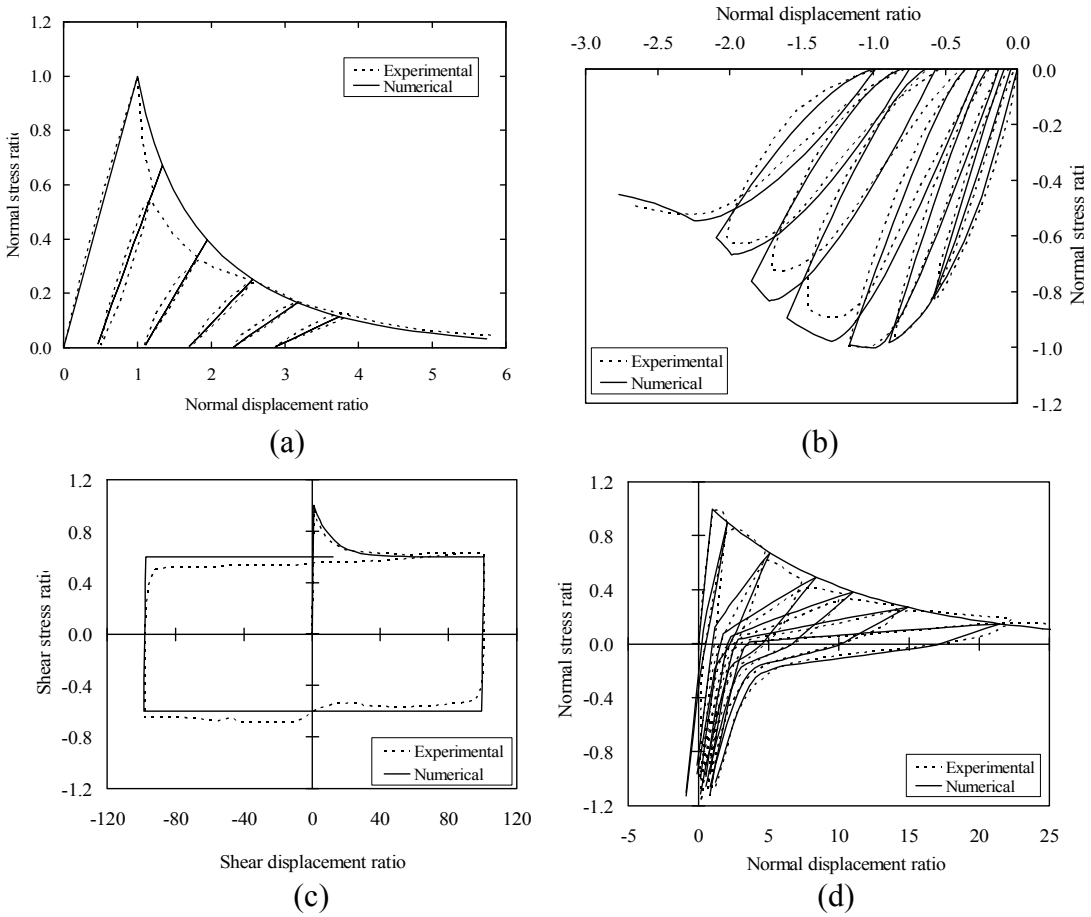

Figure 7: Comparison between experimental and numerical results for uniaxial testing: (a) tension; (b) compression; (c) shear; (d) tension-compression.

It was found that the geometric asymmetry in the micro-structure (arrangement of the units) influenced significantly the structural behaviour of the wall. Note that, depending in the loading direction, the masonry course starts either with a full unit or only with half unit. Figure 8a shows that the monotonic collapse load is 112.0 kN in the LR direction and 90.8 kN in the RL direction, where L indicates left and R indicates right. The cyclic collapse load is 78.7 kN, which represents a loss of ~13% with respect to the minimum monotonic value but a loss of ~30% with respect to the maximum monotonic value. This demonstrates the importance of cyclic loading but also the importance of taking into account the micro-structure. It is also clear from these analyses that masonry shear walls with diagonal zigzag cracks possess an appropriate seismic behaviour with respect to energy dissipation, see Figure 8b.

Figure 8c presents the results of a high wall, which simply rocks in both ways. The highly non-linear shape of the load-displacement curve is essentially due to the opening and subsequent closing, under load reversal, of the top and bottom bed joints. Similar deformed patterns, involving the opening of extreme bed joints, were observed during the experimental test. Numerical results show that the cyclic behaviour of the wall is controlled by the opening and closing of the extreme bed joints, where damage is mainly concentrated, see Figure 8d. The model also shows

low energy dissipation, which is a consequence of the activated non-linear mechanism (opening-closing of joints). As shown, the failure of this wall is much different from the previous wall, stressing the relevance of the internal structure.

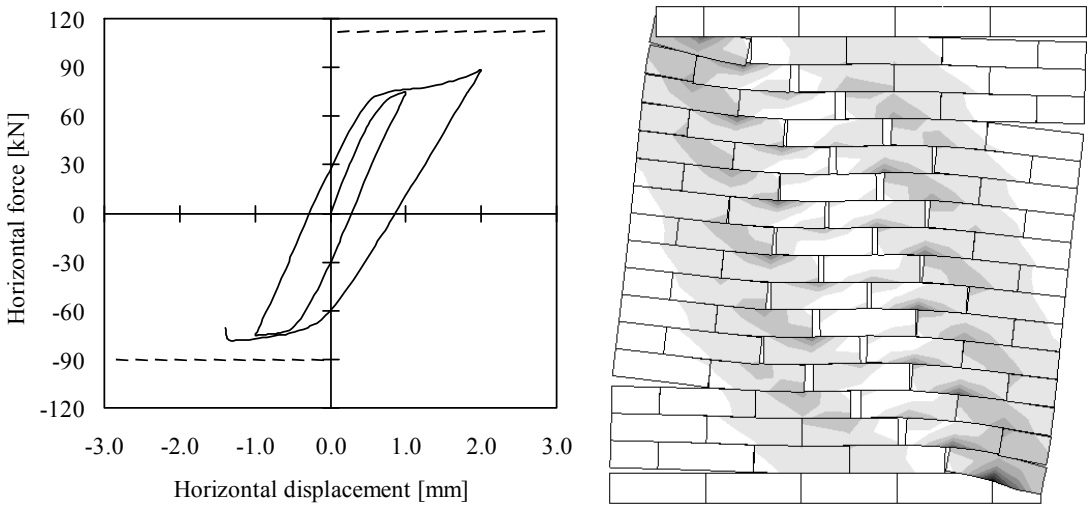

(a)

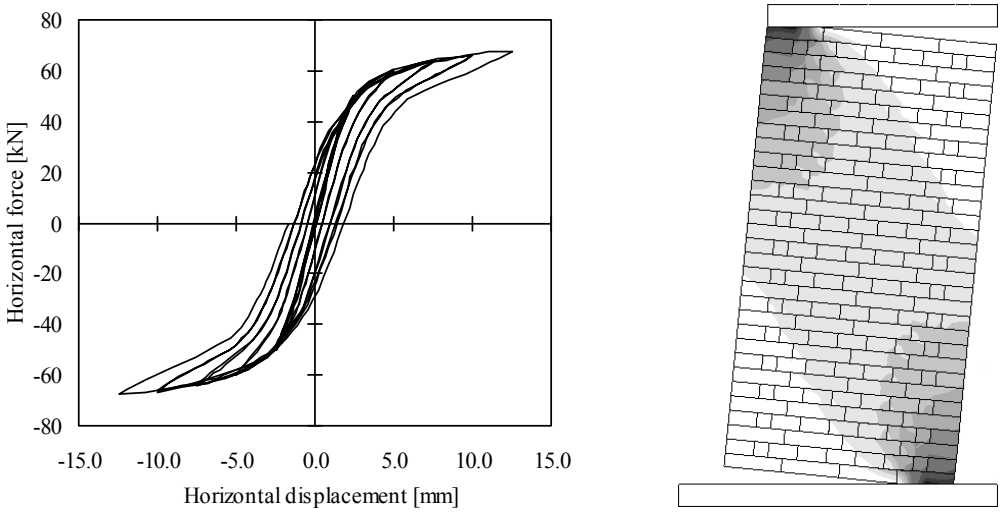

(b)

Figure 8: Results obtained with interface cyclic loading model for shear walls, in terms of force-displacement diagram and failure mode: (a) wall failing in shear; (b) wall failing in bending.

3.2 Homogenization

The approach based on the use of averaged constitutive equations seems to be the only one suitable to be employed a large scale finite element analyses, Lourenço [9,10]. Two different approaches are illustrated in Figure 9, one collating experimental date at average level and another from homogenization techniques. A major difference is that homogenization techniques provide continuum average

results as a mathematical process that include the information on the micro-structure. Average information, namely a continuum failure surface is not known, even if it can be calculated for different stress paths.

The complex geometry of the masonry representative volume, i.e. the geometrical pattern that repeats periodically in space, means that no closed form solution of the problems exists for running bond masonry. One of the first ideas presented was to substitute the complex geometry of the basic cell with a simplified geometry, so that a closed-form solution for the homogenization problem was possible. This approach, rooted in geotechnical engineering applications, assumed masonry as a layered material, see Lourenço [11] for a matrix formulation, and a so called "two-step homogenization". In the first step, a single row of masonry units and vertical mortar joints were taken into consideration and homogenized as a layered system. In the second step, the "intermediate" homogenized material was further homogenized with horizontal joints in order to obtain the final material. This simplification does not allow to include information on the arrangement of the masonry units with significant errors in the case of non-linear analysis. Moreover, the results depend on the sequence of homogenization steps.

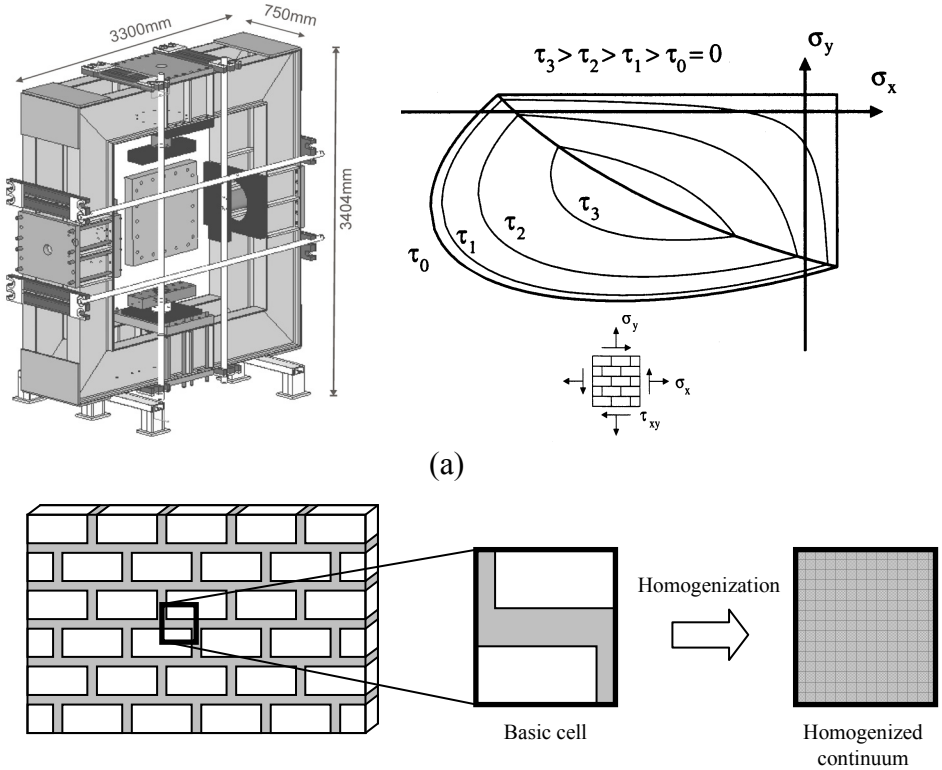

Figure 9: Constitutive behaviour of materials with micro-structure: (a) collating experimental data and defining failure surfaces; (b) a mathematical process that uses information on geometry and mechanics of components.

To overcome the limitations of the two-step homogenization procedure, micro-mechanical homogenization approaches that consider additional internal

deformation mechanisms have been derived, e.g. Zucchini and Lourenço [12,13]. The implementation of these approaches in standard macroscopic finite element non-linear codes is simple and the approaches can compete favourably with macroscopic approaches, see Lourenço at al. [14] for a review.

Here, a micro-mechanical model for the limit analysis for masonry is briefly reviewed [15,16]. In the model, the elementary cell is subdivided along its thickness in several layers. For each layer, fully equilibrated stress fields are assumed, adopting polynomial expressions for the stress tensor components in a finite number of sub-domains. The continuity of the stress vector on the interfaces between adjacent sub-domains and suitable anti-periodicity conditions on the boundary surface are further imposed. In this way, linearized homogenized surfaces in six dimensions for masonry in- and out-of-plane loaded are obtained. Such surfaces are then implemented in a finite element limit analysis code for simulation of 3D structures, and including, as recent advances, blast analysis and quasi-periodic masonry internal structure.

3.2.1 Homogenized Failure Surfaces

Figure 10 shows a masonry wall constituted by a periodic arrangement of bricks and mortar arranged in running bond. For a general rigid-plastic heterogeneous material, homogenization techniques combined with limit analysis can be applied for the evaluation of the homogenized in- and out-of-plane strength domain. In the framework of perfect plasticity and associated flow rule for the constituent materials, and by means of the lower bound limit analysis theorem, S^{hom} can be derived by means of the following (non-linear) optimization problem:

$$S^{\text{hom}} = \left\{ \max(\mathbf{M},\mathbf{N}) \,|\, \left\{ \begin{array}{rl} \mathbf{N} = \dfrac{1}{|Y|}\displaystyle\int_{Y\times h} \boldsymbol{\sigma} dV & (a) \\ \mathbf{M} = \dfrac{1}{|Y|}\displaystyle\int_{Y\times h} y_3 \boldsymbol{\sigma} dV & (b) \\ div\boldsymbol{\sigma} = \mathbf{0} & (c) \\ [\![\boldsymbol{\sigma}]\!]\mathbf{n}^{\text{int}} = \mathbf{0} & (d) \\ \boldsymbol{\sigma}\mathbf{n} \quad \text{anti-periodic} \quad \text{on} \quad \partial Y_l & (e) \\ \boldsymbol{\sigma}(\mathbf{y}) \in S^m \quad \forall \mathbf{y} \in Y^m \;;\; \boldsymbol{\sigma}(\mathbf{y}) \in S^b \quad \forall \mathbf{y} \in Y^b & (f) \end{array} \right\} \right\} \qquad (7)$$

where:

- $\mathbf{N}$ and $\mathbf{M}$ are the macroscopic in-plane (membrane forces) and out-of-plane (bending moments and torsion) tensors;
- $\boldsymbol{\sigma}$ denotes the microscopic stress tensor;
- $\mathbf{n}$ is the outward versor of ∂Y_l surface;
- $[\![\boldsymbol{\sigma}]\!]$ is the jump of micro-stresses across any discontinuity surface of normal $\mathbf{n}^{\text{int}}$;
- S^m and S^b denote respectively the strength domains of mortar and bricks;

- Y is the cross section of the 3D elementary cell with $y_3 = 0$, $|Y|$ is its area, V is the elementary cell volume, h represents the wall thickness and $\mathbf{y} = (y_1 \quad y_2 \quad y_3)$ are the assumed material axes;
- Y^m and Y^b represent mortar joints and bricks respectively.

In order to solve Equations (7) numerically, an admissible and equilibrated micro-mechanical model is adopted, Milani et al. [15]. The unit cell is subdivided into a fixed number of layers along its thickness, as shown in Figure 10b. For each layer in the wall thickness direction, one-fourth of the representative volume element is sub-divided into nine geometrical elementary entities (sub-domains), so that the entire elementary cell is sub-divided into 36 sub-domains.

For each sub-domain (k) and layer (L), polynomial distributions of degree (m) in the variables (y_1, y_2) are a priori assumed for the stress components. For out-of-plane actions the proposed model requires a subdivision of the wall thickness into several layers, with a fixed constant thickness for each layer.

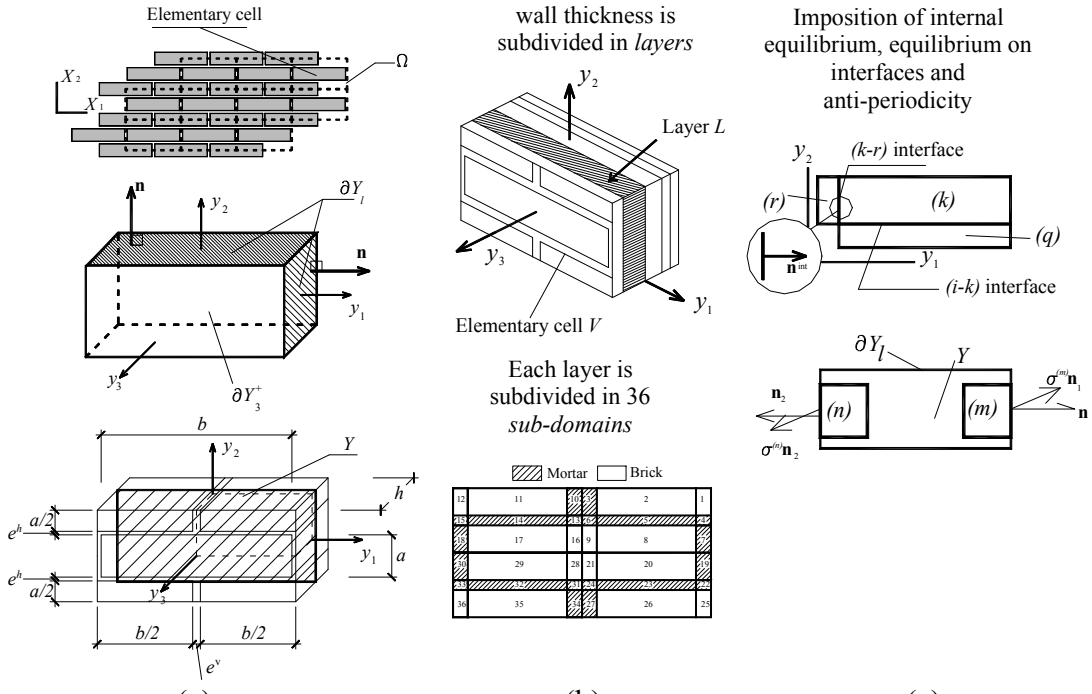

Figure 10: Proposed micro-mechanical model: (a) elementary cell; (b) subdivision in layers along thickness and subdivision of each layer in sub-domains; (c) imposition of internal equilibrium, equilibrium on interfaces and anti-periodicity.

3.2.2 Examples of Application

The homogenized failure surface obtained with the above approach has been coupled with finite element limit analysis. Both upper and lower bound approaches

have been developed, with the aim to provide a complete set of numerical data for the design and/or the structural assessment of complex structures. The finite element lower bound analysis is based on an equilibrated triangular element, while the upper bound is based on a triangular element with discontinuities of the velocity field in the interfaces. Recent developments include the extension of the model to blast analysis, Milani et al. [17], and to quasi-periodic masonry, Milani and Lourenço [18].

An enclosure running bond masonry wall subjected to a distributed blast pressure is considered first. The wall is supposed simply supported at the base and on vertical edges, whereas the top edge is assumed unconstrained, due to the typical imperfect connection between infill wall and RC beam. A full 3D FE heterogeneous elastic-plastic dynamic analysis has been also conducted, in order to have a deep insight into the problem and to collect alternative data to compare the results with those provided by the present rigid-plastic approach. For the 3D model, a rigid infinitely resistant behavior for bricks was assumed, whereas for joints a Mohr-Coulomb failure criterion with the same tensile strength and friction angle used in the homogenised approach for joints was adopted. Eight-noded brick elements were utilized both for joints and bricks, with a double row of elements along wall thickness.

A comparison between the deformed shapes at t=400 msec obtained with the present model and the commercial software is schematically depicted in Figure 11a,b. As it is possible to notice, the models give almost the same response in terms of deformed shape for the particular instant time inspected, confirming that reliable results may be obtained with the model proposed. On the other hand, it is worth underlining that the homogenized rigid plastic model required only 101 seconds to be performed on a standard PC Intel Celeron 1.40 GHz equipped with 1Gb RAM, a processing time around 10^{-3} lower than the 3D case. Comparisons of time-maximum displacement diagrams provided by the two models analyzed is reported in Figure 11c, together with the evolution of the deformation provided by the homogenized model proposed.

Recently, in Milani and Lourenço [18] two different classes of problems have been investigated, the first consisting of full stochastic representative element of volume (REV) assemblages without horizontal and vertical alignment of joints, the second assuming the presence of a horizontal alignment along bed joints, i.e. allowing blocks height variability only row by row. The model is characterized by a few material parameters and it is therefore particularly suited to perform large scale Monte Carlo simulations. Masonry strength domains are obtained equating the power dissipated in the heterogeneous model with the power dissipated by a fictitious homogeneous macroscopic plate. A stochastic estimation of out-of-plane masonry strength domains (both bending moments and torsion are considered) accounting for the geometrical statistical variability of blocks dimensions is obtained with the proposed model. The case of deterministic block height (quasi-periodic texture) can be obtained as a subclass of this latter case. As an important benchmark, the case in which joints obey a Mohr-Coulomb failure criterion is also tested and compared with results obtained assuming a more complex interfacial behaviour for mortar.

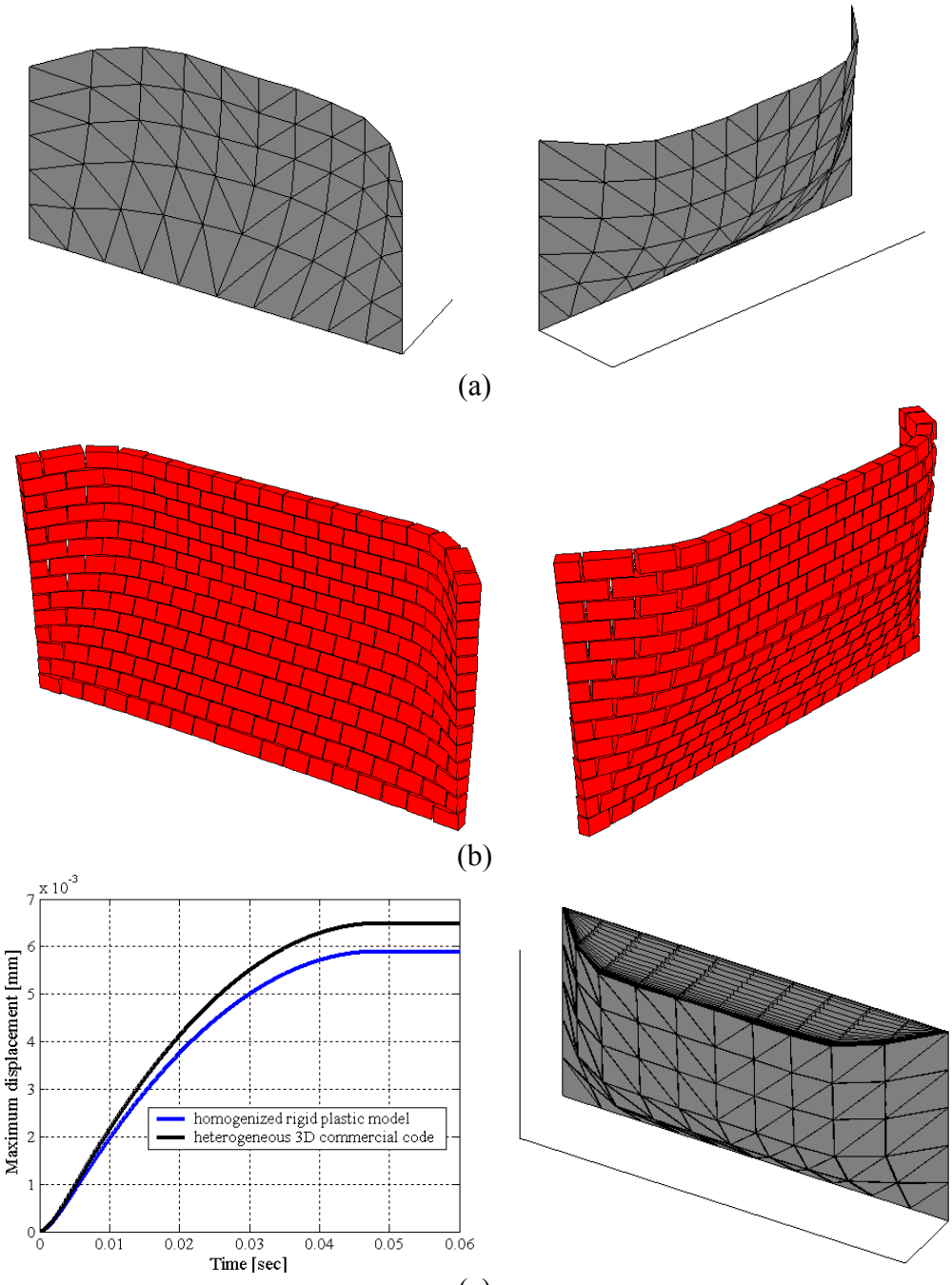

Figure 11: Masonry infill wall subjected to blast pressure: Comparison among deformed shapes at t = 400 msec for (a) Homogenized limit analysis approach and (b) heterogeneous 3D elastic-plastic FE approach; (c) comparison between maximum out of plane displacements and limit analysis failure mode.

In order to show the capabilities of the approach proposed when dealing with large scale structures, the ultimate behaviour prediction of a Romanesque masonry church façade located in Portugal. Comparisons with finite element heterogeneous approaches and "at hand" calculations show that reliable predictions of the load

bearing capacity of real large scale structures may be obtained with a very limited computational effort, see Figure 12.

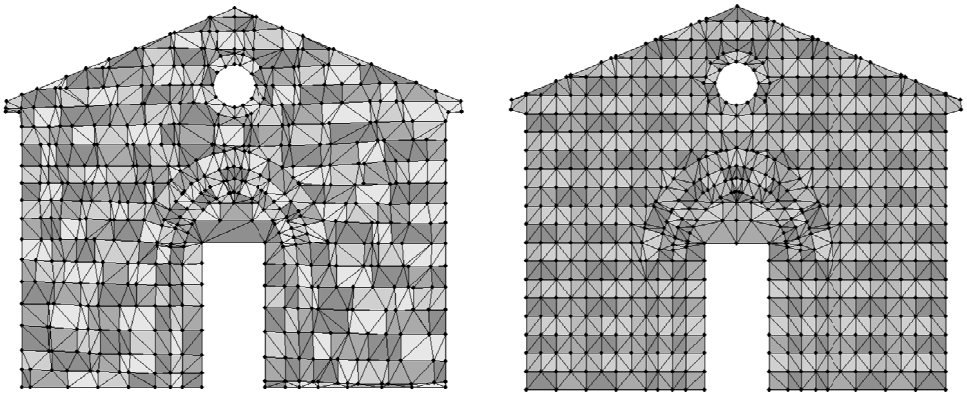

(a)

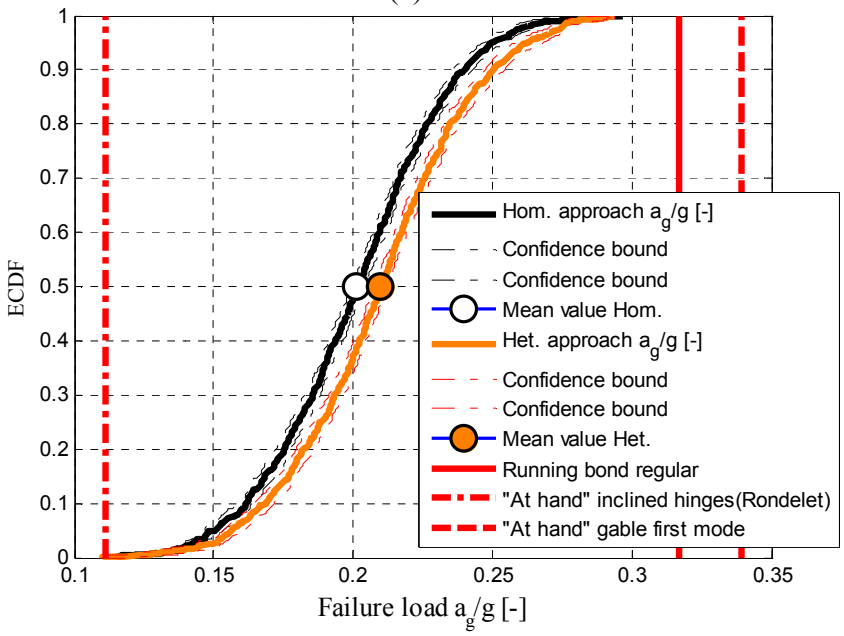

(b)

Figure 12: Church of Gondar, FE discretization adopted: (a) heterogeneous random mesh vs. mesh for running bond regular heterogeneous and homogenized random analysis; (b) ECDF of the failure load provide through a direct heterogeneous approach and homogenized limit analysis simulations, including deterministic values found using hand failure mechanisms and assuming a running bond.

4 Solving Engineering Problems

The safety assessment of historical masonry constructions is a complex task, due to many factors, such as: geometry data is missing; information about the inner core of the structural elements is also missing; characterization of the mechanical properties of the materials used is difficult and expensive; large variability of mechanical properties, due to workmanship and use of natural materials; significant changes in

the core and constitution of structural elements, associated with long construction periods; construction sequence is unknown; existing damage in the structure is unknown; regulations and codes are non-applicable. Lourenço [19] addresses the possibilities and relevance of advanced computations.

Monastery of Jerónimos is, probably, the crown asset of Portuguese architectural heritage. The construction of the monastery started in 1499 or 1500. The monastery is built with limestone (usually denoted by "lioz" type) quarried locally. The monumental set has considerable dimensions in plan, more than 300×50 m^2, and an average height of 20 m (50 m in the towers), see Figure 13. The monastery is arranged around two courts.

Several different analyses have been carried out in this monastery, see Lourenço et al. [20] and Roque [21] for more information. The analysis were carried out sequentially, taking into consideration the data available, the sought information and the available budget for structural assessment.

4.1 Global Structural Analysis of the Compound

The first analysis carried out focused in the behaviour of the full monastery compound under seismic loading. For this purpose, non-linear static (pushover) analysis was adopted. Pushover analysis is a non-linear static analysis carried out under conditions of constant gravity loads and monotonically increasing horizontal loads. In the complete model only the very large openings were considered. The geometry of the model was referred to the average surfaces of the elements. All the walls, columns, buttresses, vaults and towers were included in the model, with the exception of a few minor elements. All elements possess quadratic displacement fields. The mesh includes around 8000 elements, 23500 nodes and 135000 degrees of freedom. The time-effort necessary for total mesh generation, including definition of supports, loads and thicknesses, can be estimated in three man-months.

For the safety assessment, five independent push-over non-linear analyses were carried out, namely for vertical loads and for seismic loading along two directions (with positive and negative sign). Figure 13b shows the deformed mesh for seismic loading along the transversal direction to the church nave. It can be seen that the towers of the Museum are the critical structural elements featuring displacements of around 0.10 m in each case and a maximum crack width of around 0.01 m. The maximum compressive stresses reach values up to 4.0 N/mm^2. These values are very localized in the buttresses, in one of the bodies adjacent to the monument and in the arcade. Given the fact that this is an accidental loading condition and that the stresses are localized, it is assumed that the structure is not at risk. The average maximum values are around 2.0-2.5 N/mm^2, which seem acceptable.

4.2 Detailed Structural Analysis of the Church (Gravity Load)

The columns of the church are very slender and exhibit moderate out-of-plumbness. As the model previously adopted for the church was very simplified and the vaults were not adequately represented, more refined models have been adopted for a new study of the church under vertical and earthquake loading.

(a)

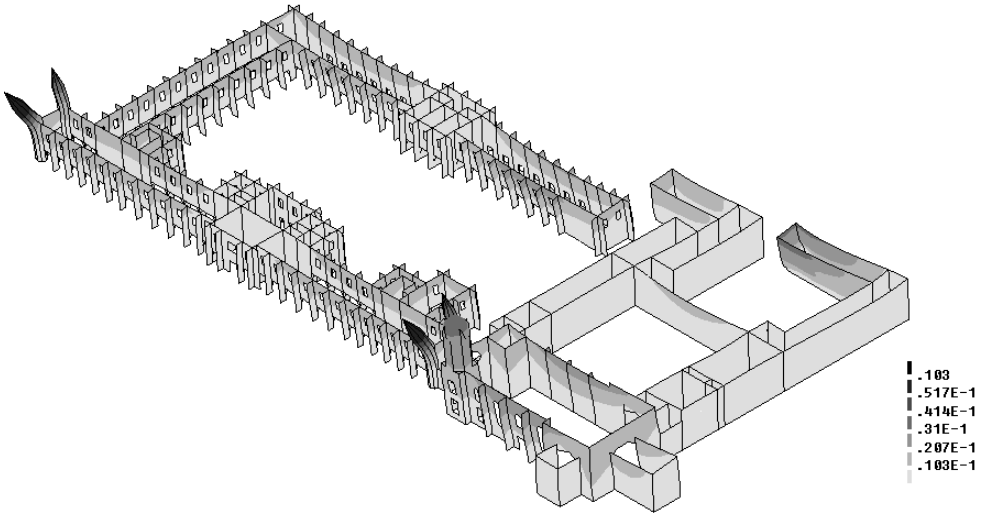

(b)

Figure 13: Monumental set of Monastery of Jerónimos: (a) aerial view; (b) deformed meshes and contour of maximum displacements for seismic load along the transversal Z axis of the model

The church has considerable dimensions, namely a length of 70 m, a width of 40 m and a height of 24 m. The plan includes a single bell tower (south side), a single nave, a transept, the chancel and two lateral chapels. The south wall has a thickness of around 1.9 m and possesses very large openings. Three large trapezoidal buttresses ensure the stability of the wall. The north wall is extremely robust (with an average thickness of around 3.5 m). This wall includes an internal staircase that provides access to the cloister. The chancel walls are also rather thick (around 2.5-2.65 m). The nave is divided by two rows of columns, with a free height of around 16.0 m. Each column possesses large bases and fan capitals. The

transverse sections of the octagonal columns have a radius of 1.04 m (nave) and 1.88 m (nave-transept). The columns seem to be made of a single block or two blocks, for the nave, and four blocks, for the transept. The vaults are ribbed and are connected to the columns by large fan capitals. Cross section of the nave vault is, mostly, a slightly curved barrel vault, even if supported at the columns. Thin stone slabs are placed on top of the stone ribs. On top of the slabs, a variable thickness mortar layer exists. The part of the slab inside the capital is filled with a concrete-like material with stones and clay mortar. On top of the vaults, brick masonry wallets were built during the 1930's to provide support for the roofing tiles.

The adopted model for the main nave includes the structural detail representative of the vault under the most unfavourable possibility, see Figure 14a, using symmetric boundary conditions. Therefore, the model represents adequately the collapse of the central-south part of the nave. The model includes three-dimensional volume elements, for the ribs and columns, and curved shell elements, for the infill and stones slabs, see Figure 14b. The external (south) wall was represented by beam elements, properly tied to the volume elements. The supports are fully restrained, being rotations possible given the non-linear material behaviour assumed. All elements have quadratic interpolation, resulting in a mesh with 33335 degrees of freedom. The time-effort necessary for total mesh generation, including definition of supports, loads and thicknesses, can be estimated in three man-months.

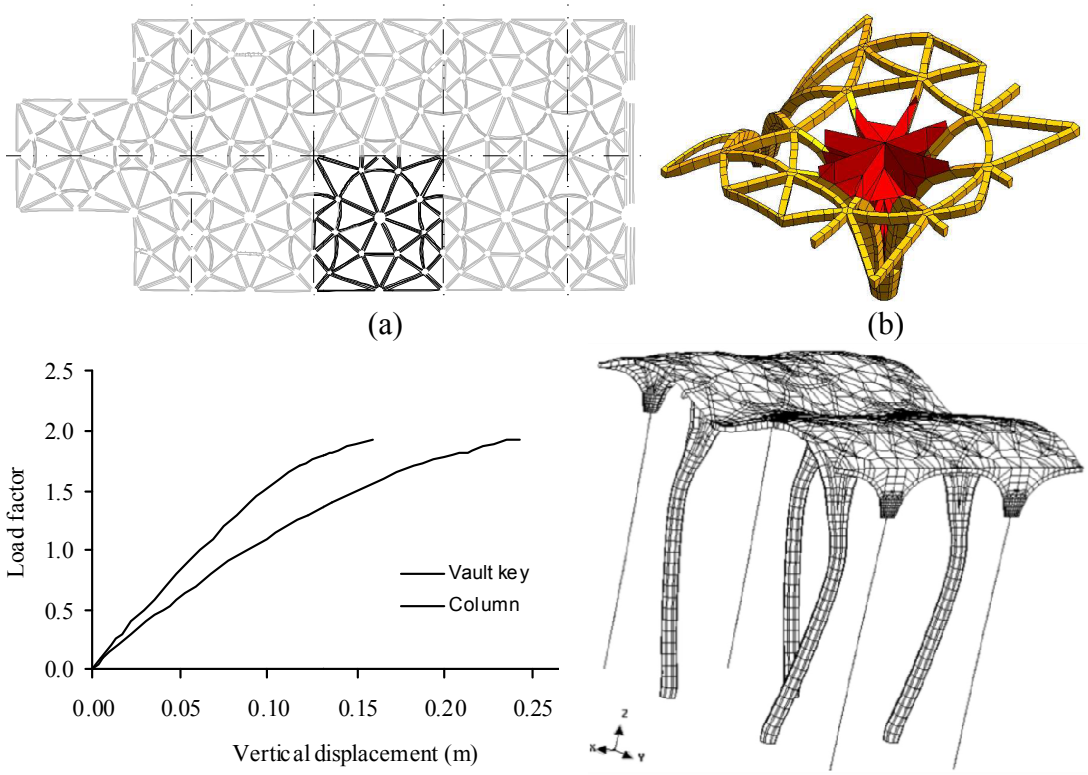

Figure 14: Detailed model of the church for vertical loading: (a) church plan and basic plan; (b) details around capital; (c) load-displacement diagram; (d) incremental deformed mesh at failure

The actions considered in the analysis include only the self-weight of the structure. Figure 14c illustrates the load-displacement diagrams for the vault key and top of the column. Here, the load factor represents the ratio between the self-weight of the structure and the applied load. It is possible to observe that the response of the structure is severely nonlinear from the beginning of loading, for the nave, and from a load factor of 1.5, for the column. The behaviour of the nave is justified by the rather high tensile stresses found in the ribs, using a linear elastic model. The collapse of the columns is due to the normal and flexural action.

The deformed mesh at failure, see Figure 14d, indicates that the structural behaviour is similar to a two-dimensional frame, with a collapse mechanism of five hinges (four hinges at the top and base of the columns and one at the key of the vault. The compressive strength of the columns controls the safety of the church for vertical loading. Nevertheless, there is some vault effect with slightly larger displacements at the central octagon, formed between the four capitals. The stresses are bounded in tension and compression, meaning that cracking and crushing occurs.

4.3 Detailed Structural Analysis of the Church (Earthquake Load)

For the seismic analysis of the church, a simplified model using beam elements was used, with a total of 25452 degrees of freedom, see Figure 15a. The time-effort necessary for total mesh generation, including definition of supports, loads and thicknesses, can be estimated in three man-months. This model was subjected to push-over analyses and time integration. The time for analysis and testing different retrofitting techniques can be estimated in nine man-months.

Initially the model was validated using modal identification, as well as a comparison with the previous detailed model for gravity loading. Subsequently, pushover analyses parallel and perpendicular to the nave of the church were carried out. Figure 15b-f shows results in terms of seismic load vs. selected horizontal displacements, failure mechanism in the finite element model and virtual collapse mechanisms. The results indicated that the columns are again much relevant for the collapse of the nave, with eccentric compression and cracking. The weakest mechanism for the seismic loading is the transverse one involving collapse for the non-constrained side of the nave, but only with 10% difference with respect the collapse to the cloister side. Still, adequate global strength seems to be found.

In order to further validate these observations and discuss the damage introduced by an earthquake, non-linear time integration analyses were carried out, see Figure 15g for the typical results involving collapse of one of the columns. The results indicate that no local or total collapse is to be expected for a 475 or 975 years return period (yrp) earthquake. Collapse is obtained for a 5000 yrp earthquake, with collapse of the northern columns of the nave (on the side of the cloister), together with the collapse of the bell tower.

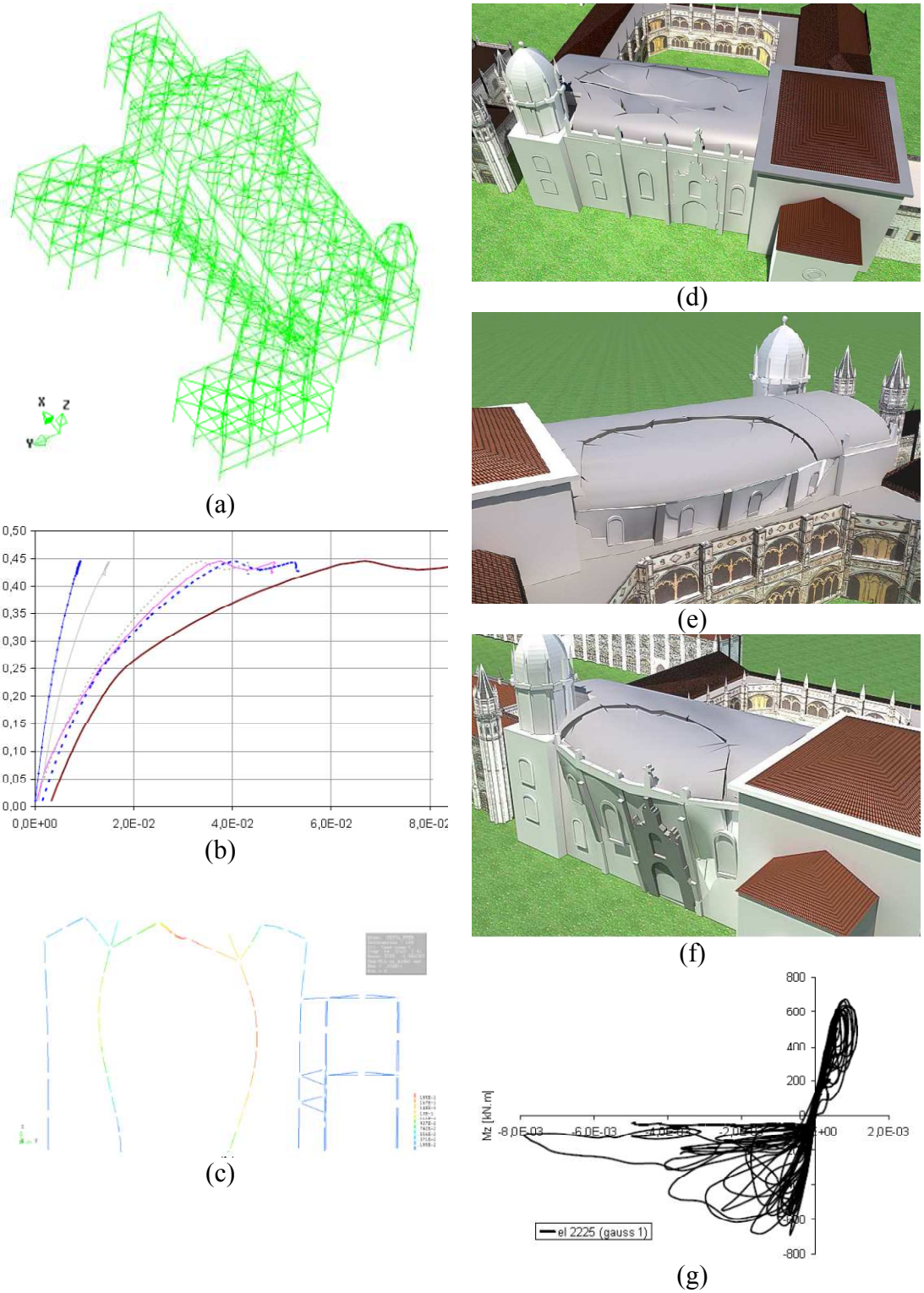

Figure 15: Detailed model of the church for horizontal loading: (a) finite element mesh; (b) push-over results, seismic action vs. displacement at given nodes; (c) example of failure mechanism; (d) virtual collapse mechanisms for different push-over analyses; (e) example of column response for time integration analysis.

5 Conclusions

Constraints to be considered in the use of advanced modelling are the cost, the need of an experienced user / engineer, the level of accuracy required, the availability of input data, the need for validation and the use of the results.

As a rule, advanced modelling is a necessary means for understanding the behaviour and damage of masonry constructions. Micro-modelling techniques for masonry structures allow a deep understanding of the mechanical phenomena involved. For large scale applications, average continuum mechanics must be adopted and homogenization techniques represent a popular and active field in masonry research. An example of an outstanding cultural heritage building is provided here, showing how different modelling strategies can be used to assess structural safety.

References

[1] P.B. Lourenço, L.F. Ramos, "Characterization of the cyclic behavior of dry masonry joints", Journal of Structural Engineering, ASCE, 130(5), 779-786, 2004.

[2] G. Vasconcelos, P.B. Lourenço, "In-plane experimental behavior of stone masonry walls under cyclic loading", Journal of Structural Engineering, ASCE, 135(10), 1269-1277, 2009

[3] J.G. Rots, "Numerical simulation of cracking in structural masonry", Heron, 36(2), 49-63, 1991.

[4] J.V. Lemos, "Discrete Element Modeling of Masonry Structures", International Journal of Architectural Heritage: Conservation, Analysis, and Restoration, 1(2), 190-213, 2007.

[5] P.B. Lourenço, J.G. Rots, "Multisurface interface model for the analysis of masonry structures", Journal of Engineering Mechanics, ASCE, 123(7), 660-668, 1997.

[6] D.V. Oliveira, P.B. Lourenço, "Implementation and validation of a constitutive model for the cyclic behaviour of interface elements", Computers & Structures, 82(17-19), 1451-1461, 2004.

[7] A. Orduña, P.B. Lourenço, "Three-dimensional limit analysis of rigid blocks assemblages. Part I: Torsion failure on frictional joints and limit analysis formulation", Int. J. Solids and Structures, 42(18-19), 5140-5160, 2005.

[8] A. Orduña, P.B. Lourenço, "Three-dimensional limit analysis of rigid blocks assemblages. Part II: Load-path following solution procedure and validation", Int. J. Solids and Structures, 42(18-19), 5161-5180, 2005.

[9] P.B. Lourenço, J.G. Rots, J. Blaauwendraad, "Continuum model for masonry: Parameter estimation and validation", Journal of Structural Engineering, ASCE, 124(6), 642-652, 1998.

[10] P.B. Lourenço, "Anisotropic softening model for masonry plates and shells", Journal of Structural Engineering, ASCE, 126(9), 1008-1016, 2000.

[11] P.B. Lourenço, “A matrix formulation for the elastoplastic homogenisation of layered materials”, Mechanics of Cohesive-Frictional Materials, 1, 273-294, 1996.
[12] A. Zucchini, P.B. Lourenço, “A micromechanical model for the homogenisation of masonry”, International Journal of Solids and Structures, 39(12), 3233-3255, 2002.
[13] A. Zucchini, P.B. Lourenço, “Validation of a micro-mechanical homogenisation model: Application to shear walls”, International Journal of Solids and Structures, 46(3-4), 871-886, 2009.
[14] P.B. Lourenço, G. Milani, A. Tralli, A. Zucchini, “Analysis of masonry structures: review of and recent trends of homogenisation techniques”, Canadian Journal of Civil Engineering, 34 (11), 1443-1457, 2007.
[15] G. Milani, P.B. Lourenço, A. Tralli, “Homogenised limit analysis of masonry walls. Part I: Failure surfaces”, Computers & Structures, 84(3-4), 166-180, 2006.
[16] G. Milani, P.B. Lourenço, A. Tralli, “A homogenization approach for the limit analysis of out-of-plane loaded masonry walls”, Journal of Structural Engineering, ASCE, 1650-1663, 2006.
[17] G. Milani, P.B. Lourenço, A. Tralli, “Homogenized rigid-plastic model for masonry walls subjected to impact”, International Journal of Solids and Structures, 46(22-23), 4133-4149, 2009.
[18] G. Milani, P.B. Lourenço, “A simplified homogenized limit analysis model for randomly assembled blocks out-of-plane loaded”, Computers & Structures, 88(11-12), 690-717, 2010.
[19] P.B. Lourenço, “Computations of historical masonry constructions”, Progress in Structural Engineering and Materials, 4(3), 301-319, 2002.
[20] P.B. Lourenço, K.J. Krakowiak, F.M. Fernandes, L.F. Ramos, “Failure analysis of Monastery of Jerónimos, Lisbon: How to learn from sophisticated numerical models?”, Engineering Failure Analysis, 14(2), 280-300, 2007.
[21] J. Roque, “Integrated methodology for the assessment and mitigation of the seismic vulnerability of historic masonry constructions: Jerónimos church as a case study” (in Portuguese), PhD Thesis, University of Minho, 2010.